Erschienen in: Journal of Optics ; 18 (2016), 5. - 05LT01
https://dx.doi.org/10.1088/2040-8978/18/5/05LT01

Controlled polar asymmetry of few-cycle and intense mid-infrared pulses

Christian Schmidt[1], Johannes Bühler[1], Bernhard Mayer[1], Alexej Pashkin[1,2], Alfred Leitenstorfer[1] and Denis V Seletskiy[1]

[1] Department of Physics and Center for Applied Photonics, University of Konstanz, Universitätsstraße 10, D 78464 Konstanz, Germany
[2] Institute of Ion Beam Physics and Materials Research, Helmholtz Zentrum Dresden Rossendorf, PO Box 510119, D 01314 Dresden, Germany

E mail: denis.seletskiy@uni konstanz.de

Abstract

We demonstrate synthesis of ultrabroadband and phase-locked two-color transients in the multi-terahertz frequency range with amplitudes exceeding 13 MV cm ^{1}. Subcycle polar asymmetry of the electric field is adjusted by changing the relative phase between superposed fundamental and second harmonic components. The resultant broken symmetry of the field profile is directly resolved via electro-optic sampling. Access to such waveforms provides a direct route for control of low-energy degrees of freedom in condensed matter as well as non-perturbative light matter interactions under highest non-resonant electric bias.

Keywords: polar asymmetry, THz, harmonic synthesis, quantum control, mid-infrared, high field, non-perturbative light matter interaction

With the availability of intense and stable femtosecond sources, precise coherent control of light matter interactions has been shifting into the focus of ultrafast science [1, 2]. This step necessitates the ability to generate tailored phase-stable optical waveforms with subcycle precision [3]. Some prominent examples constitute synthesis of single-cycle pulses [4, 5] or novel fields with symmetry-broken polarity on subperiod and envelope timescales. The most direct approach to accomplish the latter is to superimpose a fundamental field with its phase-locked second harmonic (SH), while exercising control over the relative phase between these components. Remarkably, the resultant waveforms possessing broken polar symmetry can be used to induce a non-centrosymmetric response in an otherwise inversion-symmetric medium. It has already been demonstrated that synthetic two-color pulses can be used to drastically enhance generation of THz [6 8] radiation in centrosymmetric gas plasmas via off-resonant interaction. In addition, quantum interference of one- and two-photon resonant absorption pathways enables all-optical injection of ballistic charge and spin currents in bulk [9 11] and low-dimensional [12 14] semiconductors. Together with coherent control of molecular anisotropies [15], all those examples are governed by the resulting polar asymmetry in the envelope of the hybrid pulse [12, 16 19].

On the other hand, control of the non-perturbative character of light matter interactions in gas [20 22] or solid-state [23] physics is associated with asymmetry on the subcycle timescales of the driving field this condition is also achievable via harmonic synthesis [24, 25]. A non-centrosymmetric response of the media induced by such synthetic fields can be used for generation of odd and even harmonics. Fascinatingly, a perturbative impact of a weak SH field and the associated emission of even harmonics [26] can be applied as a sensitive probe of charge carrier dynamics ensued in a high field bias of the fundamental wave [24, 27]. Very recent studies examining solid state materials have been carried out both at mid-infrared (MIR) [28] and multi-THz [29] photon energies. In the context of symmetry-broken fields, the

Konstanzer Online-Publikations-System (KOPS)
URL: http://nbn-resolving.de/urn:nbn:de:bsz:352-0-340728

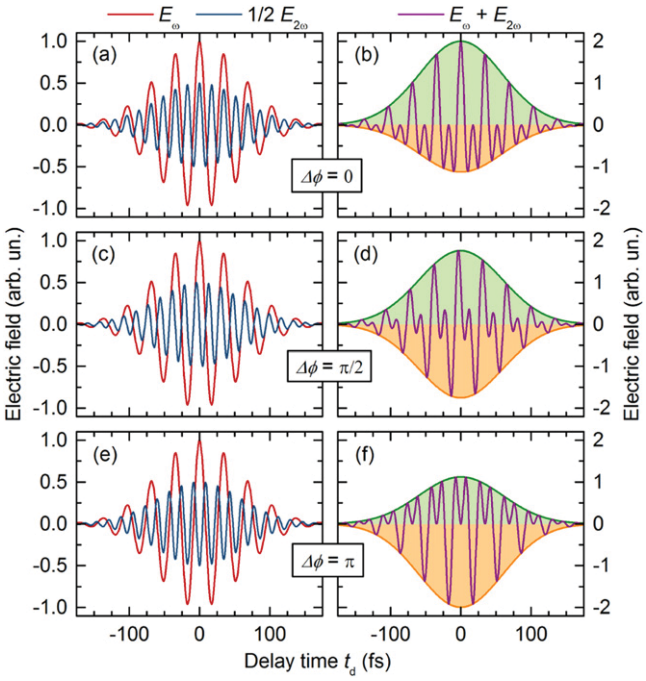

Figure 1. Calculated synthetic waveforms (right column) consisting of co polarized fundamental (30 THz, red) and second harmonic (60 THz, blue and rescaled for clarity) constituent fields (left column) for three different relative phases $\Delta\phi$ of 0 (a) and (b), $\pi/2$ (c) and (d) and π (e) and (f). Shading highlights direction of the polar asymmetry of the synthetic transient, controlled by the $\Delta\phi$ parameter.

frequency region spanning from THz to MIR is especially interesting for studies of cooperative phenomena of low energy degrees of freedom in condensed matter [30]. For such experiments it is highly desirable to combine the direct control with a precise characterization of the polar asymmetry of synthetic two-color THz waveforms.

In this letter we demonstrate generation and field-resolved detection of synthetic MIR transients with controlled polarity and peak amplitudes up to 13.9 MV cm ^{1}. Coherent superposition of fundamental and SH pulses is exploited. Adjustment of the relative phase between these two components allows for direct control of the degree of asymmetry on both the subcycle and envelope timescales.

From symmetry considerations, synthesis of a waveform with unbalanced polarity requires a superposition of a fundamental field and an even harmonic, in the simplest case the SH frequency. The total field can be represented as a sum of fundamental (amplitude E_1 at the carrier angular frequency ω) and SH (E_2) components

$$E_{\mathrm{tot}} = \Re\{E_1 \mathrm{e}^{-\mathrm{i}\omega t} + \gamma E_1 \mathrm{e}^{-\mathrm{i}2\omega t}\mathrm{e}^{-\mathrm{i}\Delta\phi}\}, \qquad (1)$$

where $\gamma = E_2/E_1$ and $\Delta\phi$ define the amplitude ratio and the relative phase difference of the two fields, respectively. To illustrate this point, figure 1 depicts a calculated E_{tot} and its constituents, projected onto the same polarization state, for three representative cases of $\Delta\phi = 0$, $\pi/2$ and π. For $\Delta\phi = 0$, the synthesized field alternates between constructive and destructive coherent superposition with each successive

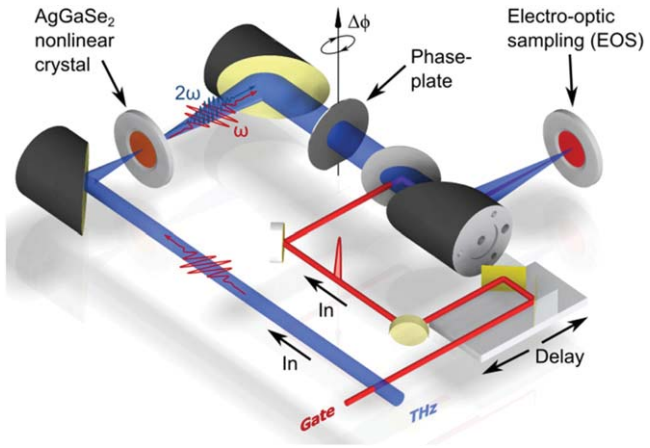

Figure 2. Experimental setup for synthetic MIR pulse generation and detection. Phase stable multi THz pulses of in plane polarization at the fundamental angular frequency ω are focused into the SH crystal ($AgGaSe_2$, type I phase matching, see text for details), generating a 2ω transient. A GaSe crystal, placed in the collimated part of the multi THz optical path, serves as a phase plate to control the relative delay between the two field constituents. An 8 fs gate pulse and a 10 μm thick $\langle 110 \rangle$ oriented ZnTe crystal enable ultrabroadband detection via electro optic sampling. The temporal offset of the gate pulse with respect to the multi THz waveform is controlled with a variable optical delay.

period of the fundamental wave. While the time-average of the field is $\langle E_{\mathrm{tot}} \rangle = 0$, the resultant waveform is nonetheless endowed with broken polar symmetry (figure 1(b)) involving, for example, a finite value of $\langle E^3_{\mathrm{tot}} \rangle$ [31]. For the $\Delta\phi = \pi/2$ case, polar symmetry is restored as both constituents are now out of phase (figure 1(d)). Finally, a relative phase $\Delta\phi = \pi$ (figure 1(f)) results in a waveform with a reversed polarity in comparison to $\Delta\phi = 0$. Thus, subcycle asymmetry can be directly manipulated by changing the relative phase between the fundamental and SH fields.

The schematic of the setup is depicted in figure 2. A frequency-doubled amplified pulse train from one of the two branches of our femtosecond Er:fiber master oscillator is used for seeding a Ti:sapphire regenerative amplifier [32]. Broadly-tunable few-μJ pulses in the multi-THz frequency range (blue beam path in figure 2) are derived by difference frequency mixing of signal beams from mutually synchronized optical parametric amplifiers pumped at 800 nm [32, 33]. A center frequency of approximately 30 THz was chosen in our experiments to ensure the possibility of broadband electro-optic sampling (EOS) of both fundamental and SH components. Frequency doubling is achieved in a 350 μm thick silver gallium selenide ($AgGaSe_2$) nonlinear crystal ($\theta = 56°$, $\varphi = 45°$) [34], placed at an intermediate focus (full width at half maximum of intensity: 60 μm) of the THz pulse train. The emerging phase-locked electric fields at carrier angular frequencies of ω and 2ω are re-collimated and transmitted through a thin dispersive plate, serving as a phase retarder for adjustment of $\Delta\phi$. In our experiment, this control element is implemented by a gallium selenide (GaSe) crystal with a thickness of 580 μm. Small azimuthal rotation of the plate introduces a relative path-length difference between the two components of the hybrid field, inducing a commensurate phase slip between them [17].

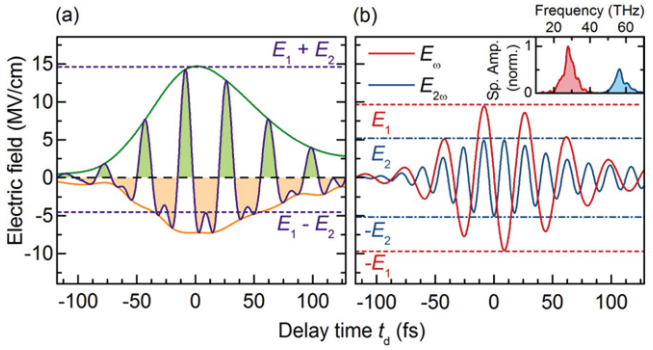

Figure 3. (a) Analysis of a synthesized two color field transient versus delay time t_d. Polar asymmetry of the electric field is highlighted with green and orange shading for positive and negative amplitudes, respectively. The peak magnitude of the resultant field of 13.9 MV cm^{-1} has been derived from the measured pulse parameters of the ω beam and the detector geometry. (b) Fundamental (centered at 28 THz) and second harmonic (56 THz) wave packets, as obtained from the inverse Fourier transform of the spectral components (inset). Color coded dashed horizontal lines mark the E_1 and E_2 maxima in the peak amplitude of the E_ω and $E_{2\omega}$ waveforms, respectively. The calculated limits of full constructive ($E_\omega + E_{2\omega}$) and destructive (E_ω $E_{2\omega}$) superpositions are depicted as dashed lines in panel (a).

The resulting synthetic waveform is monitored by an ultrabroadband EOS technique, employing a ⟨110⟩-oriented zinc telluride (ZnTe) detector crystal of a thickness of 10 μm [35, 36]. An 8 fs near-infrared sampling pulse (red beam path in figure 2) is derived from a parallel Er:fiber amplifier branch after the master oscillator [32]. We rotate the ZnTe sensor to ensure the same ratio of the detected orthogonally-polarized ω and 2ω field amplitudes as present after the SH crystal, in analogy to the effect of a linear polarizer with variable polar angle.

The measured total electric field of the two-color transient is depicted in figure 3(a). The envelope of the synthetic waveform exhibits a strong unipolar component arising from constructive superposition between positive excursions of the field cycles of the two harmonics. In particular, the positive polarity of the envelope (green solid line) is more than two times higher as compared to the one in the negative direction (orange solid line). Green and orange colors underscore the pronounced asymmetry between positive and negative polarities on subcycle timescales, respectively. Whereas the integrals over positive and negative field values within one cycle of the fundamental wave are nominally equal, the magnitudes of the extrema are different by more than a factor of two. Direct Fourier analysis identifies the spectral content of the waveform (inset in figure 3(b)) to consist of broadband fundamental (28 THz) and SH (centered at 56 THz) components. The two constituents are isolated in the spectral domain and transformed back into the time domain via a fast inverse Fourier transform (figure 3(b)). We determine the amplitude of the SH (blue solid curve) field to be approximately half as compared to the fundamental (red solid curve). This finding corresponds to an energy efficiency in SH generation of 25%, as confirmed by an ultrabroadband linear autocorrelation (not shown). From the smooth envelope shape of the measured transient in figure 3(a), we conclude negligible temporal walk-off between fundamental and SH pulses. This conclusion is in agreement with a calculation, where 35 fs walk-off resulting from group velocity mismatch suggests compatibility of our approach to harmonic synthesis with pulse durations close to single cycle. Furthermore, precise overlap between successive cycles of the two fields indicates that SH crystal and retarding wave plate introduce virtually no group velocity dispersion. Thus, optimal phase-matching conditions result in a short and intense SH pulse supporting strong polar asymmetry. It is interesting to note that the extracted peak amplitudes of E_ω and $E_{2\omega}$ (dotted lines in figure 3(b)) can be used to form the expectation bounds for perfect constructive ($E_\omega + E_{2\omega}$) and destructive ($E_\omega - E_{2\omega}$) superpositions (dotted lines in figure 3(a)) of the two fields. From equation (1), these limits are achievable only for maximally polar asymmetric waveform with $\Delta\phi = 0, \pm\pi$, which is demonstrated in figure 3(a) where $\Delta\phi \approx 0$.

Naturally, the impact of the field asymmetry depends on the nonlinear effect under study. Following the example of quantum interference currents in media with third-order nonlinear optical response [31], we define a normalized time average of the cube of the electric field as an asymmetry parameter $k = \langle E^3_{\rm tot}\rangle / \langle E^2_{\rm tot}\rangle^{3/2}$. Performing the average over the whole measured time window, the transient of figure 3(a) exhibits a k value of 0.039 for $\gamma = 0.5$. This value of the asymmetry parameter is within 94% of the maximum achievable k, calculated to occur for $\gamma = 0.7$ and $\Delta\phi = 0$. The high measured value of k highlights the level of precision in temporal matching of the components making up the combined field. The value of the asymmetry parameter can be further increased by slight adjustment of the carrier-envelope phase of the fundamental pulse, such as to ensure coincidence of the peak field with the maximum of the envelope. At this point it is also interesting to note that a prototypical single-cycle pulse, with a simulated spectrum taken by numerically filling the gap at 41 THz (inset figure 3(b)), possesses maximal k value of 0.027. It is 1.4 times lower than k of the synthetic pulse, due to a partially-destructive contribution of non-harmonic components within an octave-spanning bandwidth.

Next, we demonstrate direct manipulation of the polar asymmetry by variation of the relative phase $\Delta\phi$ between the two components with the GaSe phase plate. Figure 4 displays three traces of the total synthesized wave packets for different settings of the phase plate, corresponding to three different relative delays. Measured and calculated data for $\Delta\phi = 0$, $\pi/2$ and π are depicted. Here we focus on the subcycle structure of the synthesized field by zooming onto the central part of the multi-THz temporal profile. The change of polar asymmetry outlined in figure 1 is now implemented experimentally. One directly observes how the relative phase influences the field profile of the measured pulse: a strong unipolar peak is produced for $\Delta\phi = 0$, followed by symmetric field excursions with a cubic-like shape at zero-crossings for $\Delta\phi = \pi/2$, and finally a unipolar but reversed peak for $\Delta\phi = \pi$. Hence, the subcycle shape of the two-color waveform can be completely controlled by adjusting the relative phase $\Delta\phi$ between the two inputs. With peak fields in

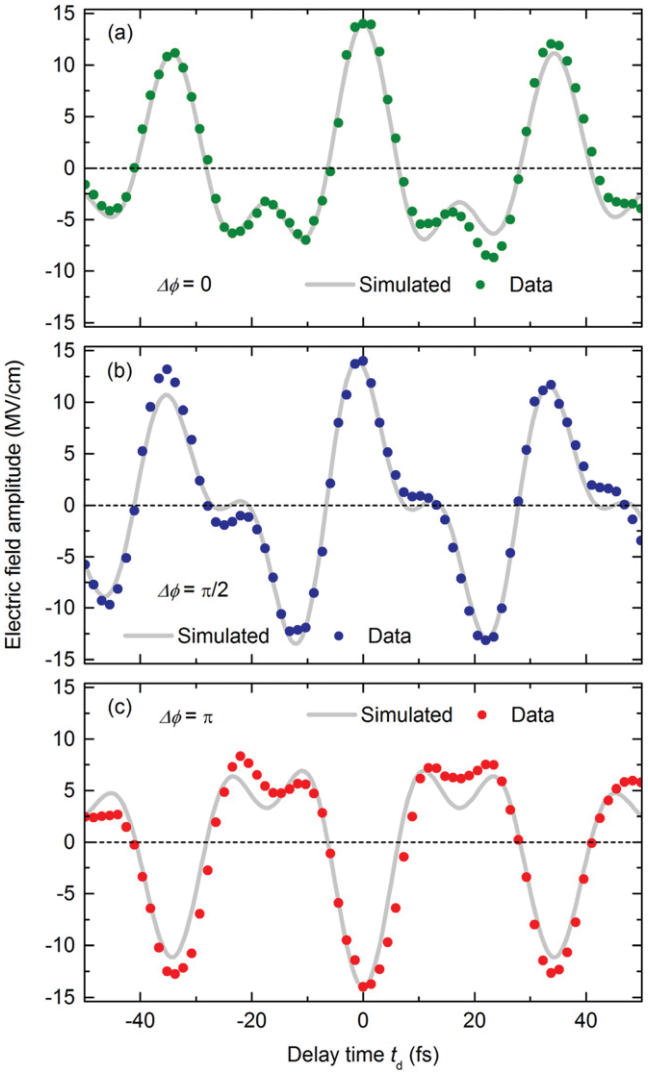

Figure 4. (a) Subcycle structure of the electric field of synthetic two color mid IR waveform for three different phase configurations. The electric field amplitude is displayed over delay time t_d for EO detected data points (colored points) and calculation following equation (1) (gray solid line). In (a) the phase difference between fundamental and SH field is set to $\Delta\phi = 0$. Whereas for (b) and (c) the relative phase is changed to $\Delta\phi = \pi/2$ and $\Delta\phi = \pi$, respectively.

excess of 13 MV cm ^{1} and synthesized polar asymmetry, such pulses are ideal candidates for optical control over charge and spin currents in materials with simultaneously allowed one- and two-photon absorption [30, 37, 38], as well as non-perturbative light matter interactions [39].

In summary, we demonstrated synthesis and field-resolved detection of intense MIR transients with controlled polar asymmetry. Collinear and efficient SH generation in $AgGaSe_2$ was exploited to achieve waveforms spanning from 20 to 70 THz. Small values of group velocity mismatch support efficient harmonic synthesis of polar asymmetric transients starting from fundamental pulses as short as few optical cycles. This offers a straight-forward method to produce envelope and field symmetry-broken pulses without the need to approach the single-cycle regime. Asymmetric and intense MIR waveforms can be readily applied for quantum control and analysis of cooperative low-energy elementary excitations in condensed matter with subcycle time resolution.

Acknowledgment

Support by the National Science Foundation (No. 1160764), by the Deutsche Forschungsgemeinschaft (Collaborative Research Center SFB767), by the Zukunftskolleg of the University of Konstanz and BW MWK RiSC Programm, by the European Research Council (Advanced Grant No. 290876 'UltraPhase'), and by the Carl Zeiss Foundation ('Programm zur Förderung des wissenschaftlichen Nachwuchses') is gratefully acknowledged.

References

[1] Junginger F, Mayer B, Schmidt C, Schubert O, Mährlein S, Leitenstorfer A, Huber R and Pashkin A 2012 Non perturbative interband response of a bulk InSb semiconductor driven off resonantly by terahertz electromagnetic few cycle pulses *Phys. Rev. Lett.* **109** 147403

[2] Günter G *et al* 2009 Sub cycle switch on of ultrastrong light matter interaction *Nature* **458** 178

[3] Mayer B, Schmidt C, Bühler J, Seletskiy D V, Brida D, Pashkin A and Leitenstorfer A 2014 Sub cycle slicing of phase locked and intense mid infrared transients *New J. Phys.* **16** 063033

[4] Krauss G, Lohss S, Hanke T, Sell A, Eggert S, Huber R and Leitenstorfer A 2010 Synthesis of a single cycle of light with compact erbium doped fibre technology *Nat. Photon.* **4** 33 6

[5] Wirth A *et al* 2011 Synthesized light transients *Science* **334** 195 200

[6] Cook D J and Hochstrasser R M 2000 Intense terahertz pulses by four wave rectification in air *Opt. Lett.* **25** 1210 2

[7] Xie X, Dai J and Zhang X C 2006 Coherent control of THz wave generation in ambient air *Phys. Rev. Lett.* **96** 075005

[8] Thomson M D, Kreß M, Löffler T and Roskos H G 2007 Broadband THz emission from gas plasmas induced by femtosecond optical pulses: from fundamentals to applications *Laser Photon. Rev.* **1** 349 68

[9] Atanasov R, Haché A, Hughes J L P, van Driel H M and Sipe J E 1996 Coherent control of photocurrent generation in bulk semiconductors *Phys. Rev. Lett.* **76** 1703 6

[10] Stevens M J, Smirl A L, Bhat R D R, Najmaie A, Sipe J E and van Driel H M 2003 Quantum interference control of ballistic pure spin currents in semiconductors *Phys. Rev. Lett.* **90** 136603

[11] Fortier T M, Roos P A, Jones D J, Cundiff S T, Bhat R D R and Sipe J E 2004 Carrier envelope phase controlled quantum interference of injected photocurrents in semiconductors *Phys. Rev. Lett.* **92** 147403

[12] Dupont E, Corkum P B, Liu H C, Buchanan M and Wasilewski Z R 1995 Phase controlled currents in semiconductors *Phys. Rev. Lett.* **74** 3596 9

[13] Faist J, Capasso F, Sirtori C, West K W and Pfeiffer L N 1997 Controlling the sign of quantum interference by tunnelling from quantum wells *Nature* **390** 589 91

[14] Ruppert C, Thunich S, Abstreiter G, Fontcuberta i Morral A, Holleitner A W and Betz M 2010 Quantum interference control of femtosecond, μA current bursts in single GaAs nanowires *Nano Lett.* **10** 1799

[15] Bidault S, Brasselet S and Zyss J 2004 Coherent control of the optical nonlinear and luminescence anisotropies in molecular thin films by multiphoton excitations *Opt. Lett.* **29** 1242
[16] Khurgin J B 1995 Generation of the terahertz radiation using $\chi^{(3)}$ in semiconductor *J. Nonlinear Opt. Phys.* **04** 163
[17] Hache A, Sipe J E and van Driel H M 1999 Quantum interference control of electrical currents in GaAs *IEEE J. Quantum Electron.* **34** 1144 54
[18] Sheik Bahae M 1999 Quantum interference control of current in semiconductors: universal scaling and polarization effects *Phys. Rev.* B **60** 257
[19] Khurgin J B 2006 Quantum interference control of electrical currents and THz radiation in optically excited zinc blende quantum well *Phys. Rev.* B **73** 033317
[20] Kling M and Krausz F 2008 Attoscience: an attosecond stopwatch *Nat. Phys.* **4** 515 6
[21] Kim J, Kim C M, Kim H T, Lee G H, Lee Y S, Park J Y, Cho D J and Nam C H 2005 Highly efficient high harmonic generation in an orthogonally polarized two color laser field *Phys. Rev. Lett.* **94** 243901
[22] Mauritsson J, Johnsson P, Gustafsson E, L'Huillier A, Schafer K J and Gaarde M B 2006 Attosecond pulse trains generated using two color laser fields *Phys. Rev. Lett.* **97** 013001
[23] Schubert O *et al* 2014 Sub cycle control of terahertz high harmonic generation by dynamical Bloch oscillations *Nat. Photon.* **8** 119 23
[24] Dudovich N, Smirnova O, Levesque J, Mairesse Y, Yu Ivanov M, Villeneuve D M and Corkum P B 2006 Measuring and controlling the birth of attosecond XUV pulses *Nat. Phys.* **2** 781 6
[25] Mashiko H, Gilbertson S, Li C, Khan S D, Shakya M M, Moon E and Chang Z 2008 Double optical gating of high order harmonic generation with carrier envelope phase stabilized lasers *Phys. Rev. Lett.* **100** 103906
[26] Vampa G, Hammond T J, Thiré N, Schmidt B E, Légaré F, McDonald C R, Brabec T and Corkum P B 2015 Linking high harmonics from gas and solids *Nature* **522** 462 4
[27] Gragossian A, Seletskiy D V and Sheik Bahae M Classical trajectories in polar asymmetric laser fields: synchronous THz and XUV emission arXiv:1409.8388
[28] Vampa G, Hammond T J, Thiré N, Schmidt B E, Légaré F, McDonald C R, Brabec T, Klug D D and Corkum P B 2015 All optical reconstruction of crystal band structure *Phys. Rev. Lett.* **115** 193603
[29] Hohenleutner M, Langer F, Schubert O, Knorr M, Huttner U, Koch S W, Kira M and Huber R 2015 Real time observation of interfering crystal electrons in high harmonic generation *Nature* **523** 572 5
[30] Muniz R A and Sipe J E 2014 Coherent control of optical injection of spin and currents in topological insulators *Phys. Rev.* B **89** 205113
[31] Chudinov N, Kapitzky Y E, Shulinov A A and Ya Zel'dovich B 1991 Interferometric phase measurements of average field cube $E^2{}_\omega E^*{}_{2\omega}$ *Opt. Quant. Electron.* **23** 1055 60
[32] Sell A, Leitenstorfer A and Huber R 2008 Phase locked generation and field resolved detection of widely tunable terahertz pulses with amplitudes exceeding 100 MV cm^{-1} *Opt. Lett.* **33** 2767 9
[33] Junginger F, Sell A, Schubert O, Mayer B, Brida D, Marangoni M, Cerullo G, Leitenstorfer A and Huber R 2010 Single cycle multiterahertz transients with peak fields above 10 MV cm^{-1} *Opt. Lett.* **35** 2645
[34] Eckardt R C, Fan Y X, Byer R L, Route R K, Feigelson R S and van der Laan J 1985 Efficient second harmonic generation of 10 μm radiation in $AgGaSe_2$ *Appl. Phys. Lett.* **47** 786
[35] Wu Q, Litz M and Zhang X C 1996 Broadband detection capability of ZnTe electro optic field detectors *Appl. Phys. Lett.* **68** 2924
[36] Leitenstorfer A, Hunsche S, Shah J, Nuss M C and Knox W H 1999 Detectors and sources for ultrabroadband electro optic sampling: experiment and theory *Appl. Phys. Lett.* **74** 1516
[37] Sun D, Divin C, Rioux J, Sipe J E, Berger C, de Heer W A, First P N and Norris T B 2010 Coherent control of ballistic photocurrents in multilayer epitaxial graphene using quantum interference *Nano Lett.* **10** 1293 6
[38] Rioux J, Burkard G and Sipe J E 2011 Current injection by coherent one and two photon excitation in graphene and its bilayer *Phys. Rev.* B **83** 195406
[39] Liu C, Reduzzi M, Trabattoni A, Sunilkumar A, Dubrouil A, Calegari F, Nisoli M and Sansone G 2013 Carrier envelope phase effects of a single attosecond pulse in two color photoionization *Phys. Rev. Lett.* **111** 123901